INERS' 24

5. ULUSLARARASI MÜHENDİSLİK ARAŞTIRMALARI SEMPOZYUMU

7-9 MART/MARCH 2024

5th INTERNATIONAL ENGINEERING RESEARCH SYMPOSIUM

Düzce Universty / Düzce –TÜRKİYE

SEMPOZYUM TAM METİN KİTABI

SYMPOSIUM FULL TEXT BOOK



DÜZCE UNIVERSITY

INERS
International Engineering
Research Symposium

www.iners.duzce.edu.tr

5. Uluslararası Mühendislik Araştırmaları Sempozyumu
07-09 Mart 2024, Düzce/Türkiye

5th International Engineering Research Symposium
07-09 March 2024, Düzce/Türkiye
ISBN: 978-625-6330-05-4

5th International Engineering Research Symposium

Proceeding Book

March 7-9, 2024
Düzce, Türkiye

ISBN
978-625-6330-05-4

www.iners.duzce.edu.tr

5. Uluslararası Mühendislik Araştırmaları Sempozyumu
07-09 Mart 2024, Düzce/Türkiye

5th International Engineering Research Symposium
07-09 March 2024, Düzce/Türkiye
ISBN: 978-625-6330-05-4

High Resolution In-Shoe Plantar Pressure Measurement System: Smart Insoles

Fatih Mert Çelebi[a], Sabri Uzuner[b], Engin Nas[c]*

[a]Düzce Üniversitesi, Mühendislik Fakültesi, Makine Mühendisliği Bölümü, Düzce/Türkiye.
[b]Düzce Üniversitesi, Mühendislik Fakültesi, Mekatronik Mühendisliği Bölümü, Düzce/Türkiye.
[c]Düzce Üniversitesi, , Makine ve Metal Teknolojileri Bölümü, Düzce/Türkiye.
***Corresponding author:** fatihcelebi.dgh@duzce.edu.tr

ABSTRACT

Certain orthopedic conditions affecting the foot and knee can alter plantar pressure distribution. Accurate measurement of plantar pressure necessitates consideration of the diverse contours formed by the foot's sole during everyday movements. Consequently, researchers have devised in-shoe plantar pressure measurement systems to address this need. However, these systems only measure pressure at 3-10 points, resulting in low resolution of the results. This study has developed an intelligent insole that does not require expert control and can be used as an in-shoe system. The developed insole provides high resolution pressure measurement from 421 points. When compared with similar studies in the literature on the basis of resolution, measurement speed and cost parameters, the developed system is found to be in an advantageous position. This study provides a high resolution solution in the field of in-shoe plantar pressure measurement and can be recommended as an important resource for biomedical research.

Keywords: *Deformity, In Shoe System, Insoles, Plantar Pressure, Velostat.*

Yüksek Çözünürlüklü Ayakkabı içi Plantar Basınç Ölçüm Sistemi: Akıllı Tabanlık

ÖZET

Ayak ve dizde oluşan bazı ortopedik rahatsızlıklar plantar basınca etki etmektedir. Plantar basıncın doğru ölçümü, günlük hareketler sırasında ayak tabanının oluşturduğu çeşitli konturların dikkate alınmasını gerektirir. Sonuç olarak araştırmacılar bu ihtiyacı karşılamak için ayakkabı içi plantar basınç ölçüm sistemleri geliştirdiler. Ancak bu sistemler basıncı yalnızca 3-10 noktada ölçmektedir ve bu da sonuçların çözünürlüğünün düşük olmasına neden olmaktadır. Bu çalışmada uzman kontrolü gerektirmeyen ve ayakkabı içi sistem olarak kullanılabilecek akıllı bir iç taban geliştirildi. Geliştirilen iç taban 421 noktadan yüksek çözünürlüklü basınç ölçümü sağlar. Çözünürlük, ölçüm hızı ve maliyet parametreleri bazında literatürdeki benzer çalışmalarla karşılaştırıldığında geliştirilen sistemin avantajlı konumda olduğu görülmektedir. Bu çalışma ayakkabı içi plantar basınç ölçümü alanında yüksek çözünürlüklü bir çözüm sunmakta olup biyomedikal araştırmalar için önemli bir kaynak olarak önerilebilir..

Anahtar Kelimeler: *Ayak İçi Sistem, Deformite, Plantar Basınç, Tabanlık, Velostat.*

I. INTRODUCTION

Foot and knee health is a critical health issue affecting individuals' quality of life [1-3]. Plantar pressure distribution represents the pressure distribution of the sole of the foot [4]. For this reason, an orthopedic disorder that may occur in knee, ankle, or foot mechanics can directly affect the plantar pressure distribution, and this difference in pressure distribution can be one of the indicators that can be used to evaluate human quality of life [5]. These orthopedic disorders, Angular Deformity [6, 7], Osteoarthritis [8], Plantar Fasciitis [9], Pes Planus [10], and Pes Cavus [9] can be given as examples.

The diagnostic process of posture disorders aims to comprehensively evaluate the patient's condition and reach a specific diagnosis [11-13]. However, expert control is needed before these methods can be used widely. The specialist check-up is based on clinical skills such as assessing the patient's symptoms, reviewing the medical history, and performing a physical examination. The specialist physician aims to diagnose accurately by considering factors such as the patient's lifestyle, genetic factors, activity level and

other health problems. However, this process can sometimes take time [14], and advanced imaging technologies may be needed to understand the conditions of various disorders more clearly. Although devices such as MRI and CT accelerate this diagnostic process, a specialist's evaluation of these images prolongs the process. In addition, although medical imaging is a quick solution for diagnosis, it cannot detect the loads caused by posture disorders.

In the literature, it has been observed that basically two different methods are used to measure plantar pressure distribution [15]. The first method is platform-based high-precision pedopowergraph [16], pedobarography [17], pedobarogram [18], EMED-400 plantar pressure system [19], etc., which require expert control. However, using these devices is often costly, leading to inequalities in healthcare access [20, 21]. The second method is in-shoe systems, which are more cost-effective and do not require specialists [22]. These systems have lower measurement accuracy than platform-based systems [23, 24]. In-shoe systems generally target the four main parts of the sole of the foot: anterior, posterior, lateral and medial [25]. In these systems, four different types of sensors are generally used: capacitive [26], resistive [27], piezoelectric [28], and piezoresistive [23]. In studies conducted to measure in-shoe plantar pressure, the number of sensors placed on the sole of the foot varies between 3-9 [29-32]. The small number of sensors reduces the measurement areas and resolution of the sole of the foot.

This study proposes a low-cost, user-friendly smart insole for in-shoe use, requiring no expert control. The intelligent insoles are designed to be easily utilized, with a slim profile of 0.6 mm for comfortable daily wear. This innovation aims to offer high-resolution pressure measurements from 421 points.

II. Material and Method

The materials used in the system implemented in this study consist of two parts. The first part is the insole, which consists of acetate, copper tape, and velostat strips. The second part is the electronic card part, which allows the reading and processing of data from the insoles.

A. Design

The insoles consist of 2 layers, upper and lower. While voltage distribution is made from the lower layer, analog data is read from the upper layer. These voltage and analog data transmissions are provided using copper tapes.

The aim is to design the insoles with a thin and flexible structure for ease of use. For this reason, copper bands and velostat are fixed on nylon and acetate. In this way, it is thought that it will not cause any discomfort during use and will also eliminate the risk of product deformation thanks to its flexible structure.

Acetate Cutting

The system design process started with acetate cutting. The acetate is cut in the shape of the foot sole to hold the insole design together without causing visual pollution. The foot sole drawing transferred to acetate was drawn according to foot size 44. Basically, the entire structure is built on this acetate. Acetate was cut into 2 pieces (bottom and top layer) by the dimensions in Figure 1.

Copper Tape Array

Copper tapes were glued onto the acetate in parallel, leaving a 2 mm gap between them. The purpose of leaving a gap is to prevent any short circuit in stretching. In addition, copper bands are arranged horizontally on the lower surface and vertically on the upper surface. In this way, the intersection points have been increased. Its symbolic representation is shown in Figure 2a, the upper surface in Figure 1a, and the lower surface in Figure 1b.



a) Copper Tape Top Surface Array



b) Copper Tape Bottom Surface Array



c) Top Surface Arrangement of Velostat Strips



d) Bottom Surface Arrangement of Velostat Strips

Figure 1. Arranging Velostat and Copper Tape Strips into Layers

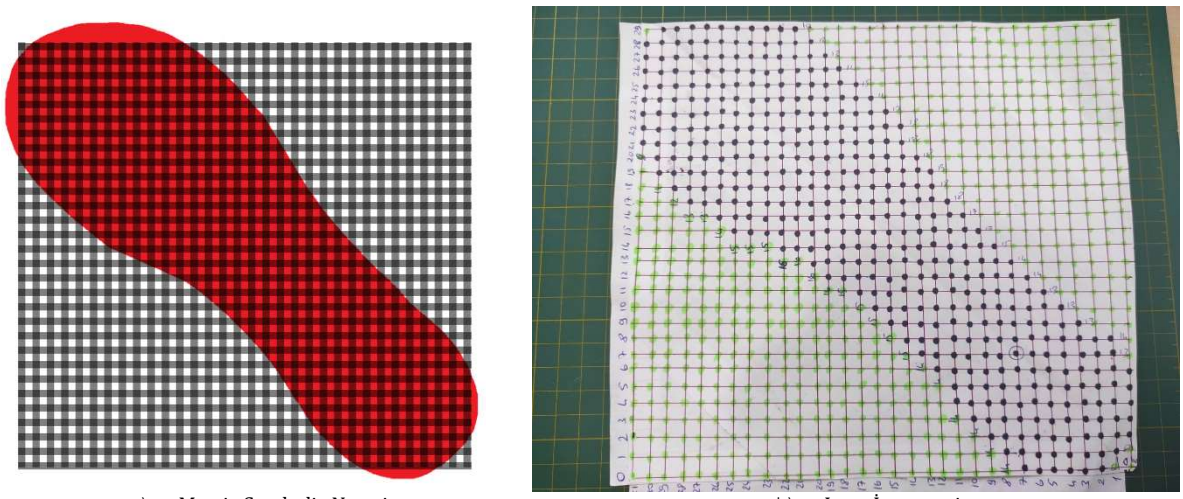
Velostat Nylon Array

Since Velostat nylons were supplied in standard sizes of 28x28 cm, they were cut to obtain 5mm thick strips. The resulting velostat nylon strips were glued onto the copper tapes on both the lower and upper surfaces. For the Velostat strips to adhere to the surface, 1 mm wide double-sided tape was added to the gaps left between the copper tapes.

Figure 1c shows the upper surface arrangement of velostat nylons, and Figure 1d shows the lower surface arrangement.

Determining Intersection Points

A total of 32 strips were obtained on the upper surface and 30 strips on the lower surface. The matrix formed by the intersection of these strips is 32x30 in size; that is, it has the capacity to accommodate 960 elements, but the matrix form was preferred for ease of data processing. For this reason, the matrix elements used in the system are the elements at the intersection of the sole of the foot. It is shown symbolically in Figure 2a.



a) Matrix Symbolic Notation b) Lane İntersections

Figure 2. Intersection Points

Intersections outside the foot sole shape are not taken into account. In the software part, the values are determined as "0".

A different intersection representation is examined in Figure 2b. Dark blue dots represent the elements to be processed, and green dots represent the elements to be defined as "0". There are 421 intersection points, each representing an independent pressure sensor.

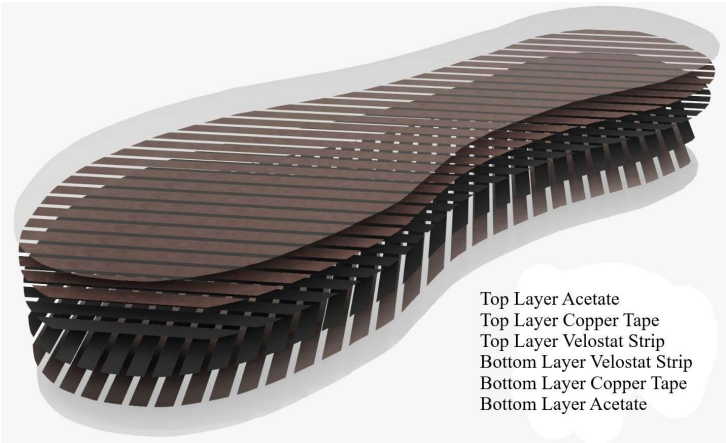


Figure 3. Detailed Insole Model

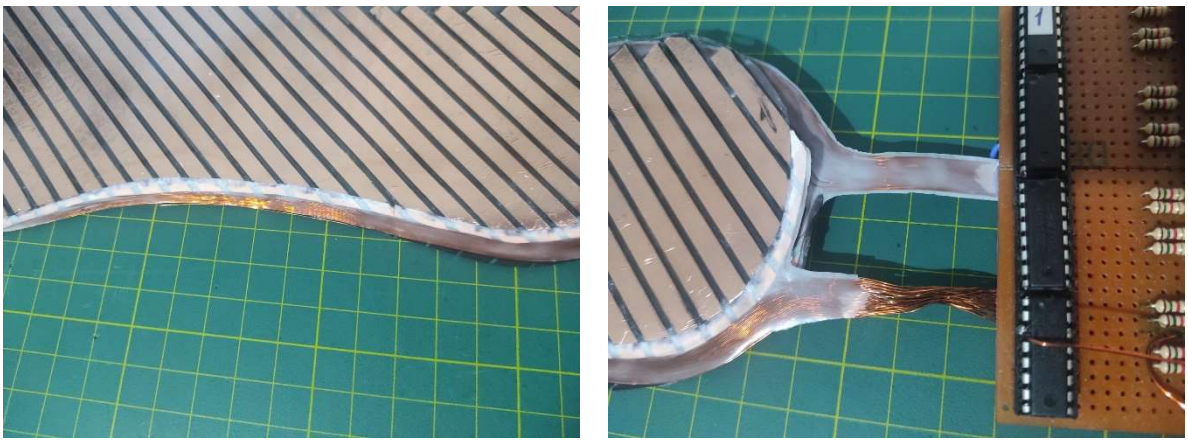
Figure 3 shows the detailed model design of the insole from the Fusion 360 program for a clear understanding of the insole design.

B. Electronic

CD4051 integrated circuit was used to read analog data using fewer pins. All read analog data is processed into matrix cells representing each pressure point. The simplified circuit diagram was designed with the Fritzing program.

Enameled Copper Wire Connection

A 0.2 mm thick enamel-coated copper wire is soldered to each of the copper tape strips in the upper and lower layers. As seen in Figure 4a, the soldered enameled copper wires are arranged side by side to form a thin layer. Then, both the solder joints and the enamel-coated copper wires are coated with UV-sensitive white resin to prevent dispersion and disconnection.



a) Enameled Copper Wire Array b) Transferring the Connections to the Circuit

Figure 4. Enameled Copper Wire Connections

After this process was applied to the upper and lower layers, all enamel-coated copper wires were transferred to the electronic circuit, as seen in Figure 4b. To avoid connection confusion, the connections of the lower and upper layers are transferred as two different paths.

In this way, while the connections are being transmitted, the high conductivity feature is preserved, and all connections are provided without any change in the thickness of the insole.

Circuit Diagram

The circuit diagram has been simplified and designed to avoid cable confusion. Detailed connection is given in the table. The ICs are listed in Figure 5, with number 1 on the left and number 8 on the right. Resistors were used in the first four integrated circuits but not in the following ones. This is because the first four integrated parts are connected to the upper layer of the insole. The upper layer is used for analog operation and the lower layer is used for digital operation. The resistors of the integrated circuits connected to the upper layer represent the simple voltage divider circuit. In order to avoid confusion, the integrated notches are arranged on the left side.

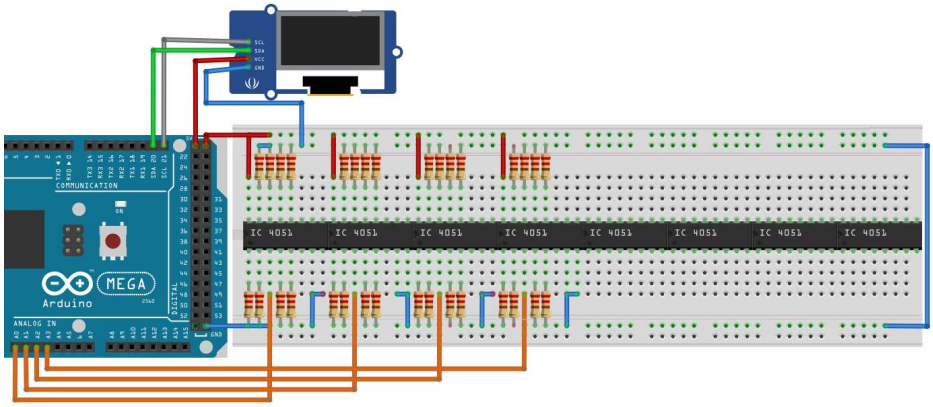


Figure 5. Circuit Diagram

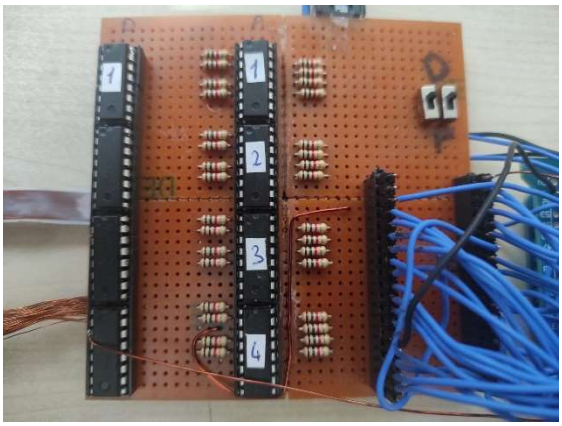
In Table 1, integrated circuits are abbreviated as "E" and numbered. The velostat strips (30 pieces) on the bottom layer of the insole are abbreviated as "IB", and the velostat strips (32 pieces) on the top layer are abbreviated as "IT". Additionally, Arduino Mega is abbreviated as “AR” and numbered using these abbreviations. In the information sheet of the CD4051 integrated circuit, the pin outputs are as follows; 1-CHANNEL I/O4, 2- CHANNEL I/O6, 3-COM OUT/IN, 4- CHANNEL I/O7, 5- CHANNEL I/O5, 6- INHIBIT, 7-VEE, 8-VSS, 9-C , 10-B, 11-A, 12- CHANNEL I/O3, 13- CHANNEL I/O0, 14- CHANNEL I/O1, 15- CHANNEL I/O2, 16-VDD. VDD and VSS pins represent the power line[33].

Table 1. Arduino Mega and Base Connection List of Circuit Board

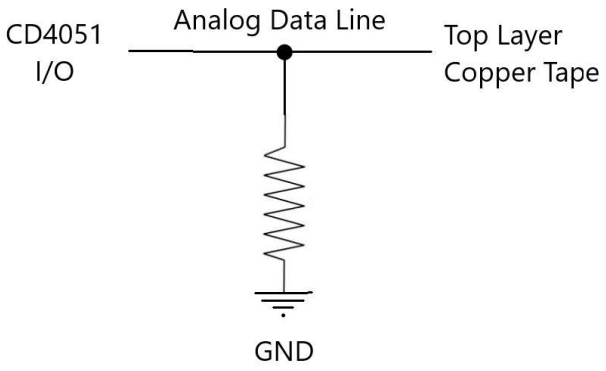
Pin Adı	E1	E2	E3	E4	E5	E6	E7	E8
Inhibit	AR34	AR35	AR36	AR37	AR53	AR52	AR51	AR50
Input A	AR22	AR25	AR28	AR31	AR38	AR41	AR44	AR47
Input B	AR23	AR26	AR29	AR32	AR39	AR42	AR45	AR48
Input C	AR24	AR27	AR30	AR33	AR40	AR43	AR46	AR49
I/O 0	IT1	IT9	IT17	IT25	IB1	IB9	IB17	IB25
I/O 1	IT2	IT10	IT18	IT26	IB2	IB10	IB18	IB26
I/O 2	IT3	IT11	IT19	IT27	IB3	IB11	IB19	IB27
I/O 3	IT4	IT12	IT20	IT28	IB4	IB12	IB20	IB28
I/O 4	IT5	IT13	IT21	IT29	IB5	IB13	IB21	IB29
I/O 5	IT6	IT14	IT22	IT30	IB6	IB14	IB22	IB30
I/O 6	IT7	IT15	IT23	IT31	IB7	IB15	IB23	-
I/O 7	IT8	IT16	IT24	IT32	IB8	IB16	IB24	-

Soldering the Electronic Circuit Board

10x10 cm perforated pertinax held the CD4051 integrated circuits, resistors and connection cables together. In Figure 6a, the 4 CD4051 integrated circuits on the right side are connected to the upper layer of the base. For this reason, all resistors are connected to the four integrated circuits on the right to act as a voltage divider circuit. The integrated circuits on the left are connected to the bottom layer, and since they are used for digital operations, no resistors are needed.



a) Electronic circuit



b) Symbolic Voltage Divider Circuit

Figure 6. Resistance Connections

Each resistor is connected to the upper layer of copper strips (32 pieces). In order to understand the voltage divider phase more clearly, Figure 6b shows a symbolic drawing of a single intersection point. Velostat Nylon also has a resistance on it. Different voltage values are obtained thanks to the fixed resistance on the circuit and the variable resistance within the velostat.

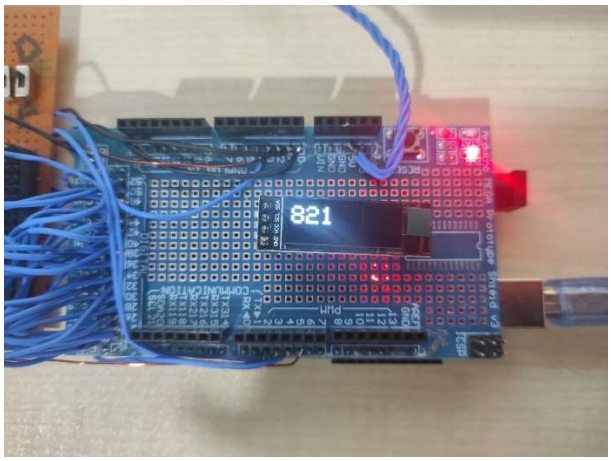


Figure 7. Arduino Connection

The integrated circuits connected to the electronic circuit's upper layer allow 32 analog data to be read from 4 pins. All control and analog pins are transmitted to Arduino Mega with a single-core assembly cable, as seen in Figure 7.

C. Software

The system software is included in Arduino Mega and is written with the Arduino IDE program. This program can be used to program all Arduino models and similar development boards containing simple microcontrollers.

Reading Data

Data reading in the system is done analogously. Thanks to Arduino Mega, 10-bit (210=1024) analog reading can be made. This reading sensitivity provides an advantage when measuring the plantar pressure distribution of individuals of higher weight or very light. Analog Reading is done from the upper insole. There are 32 strips in total on the upper insole, and each strip is connected to the CD4051 integrated circuits in 8 ways. In this way, all readings can be made from 4 analog pins. While any strip on the upper layer is being read, all strips on the lower layer (32 pieces) are powered and cut off sequentially. In this way, 30 operations were performed when reading a single strip in the upper layer, and 960 operations in total are performed when reading all strips in the upper layer. To avoid data confusion during this reading process, a waiting time of 500 us was added between each operation. In this way, all data was read in approximately 480 ms (0.48 s) without data interference. All read analog data is recorded in a 32x30 matrix.

Data Processing

All data of the 32x30 matrix was looped and listed on the serial monitor of the Arduino IDE program. Data was added to the variable called total pressure in each printing process. The total data is shown on the OLED screen, as shown in Figure 7. In this way, while all data is shown separately on the serial monitor of the Arduino IDE program, it is shown as a whole on the OLED screen.

Data Visualization

The read data is shown on the serial monitor of the Arduino IDE program as seen in Figure 8.

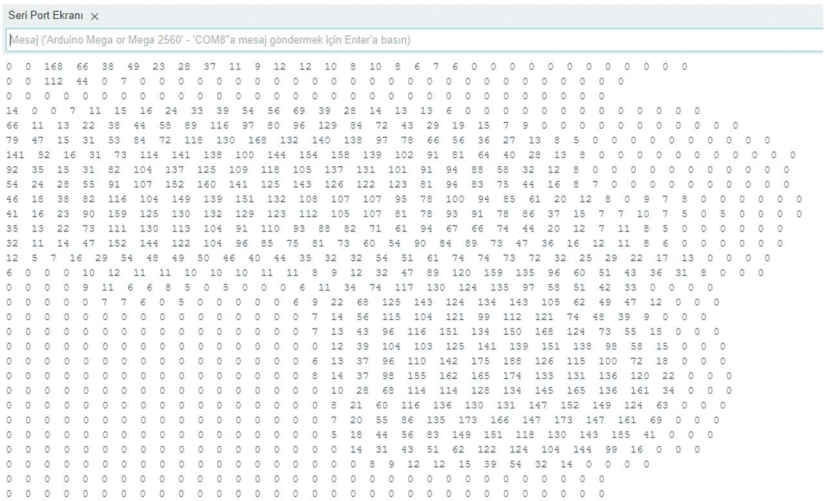


Figure 8. Serial Monitor Display

Simultaneously, total pressure data is shown on the OLED screen in Figure 7.

All data (960 pieces) displayed on the serial monitor of the Arduino IDE program were transferred to the Microsoft Excel program, each in a different cell, creating a matrix of 32x30 size. For a clearer visual understanding of the data in the Microsoft Excel program, the 0-50-200 values were colored blue-yellow-red by using the conditional formatting tool.

III. Conclusion and Discussion

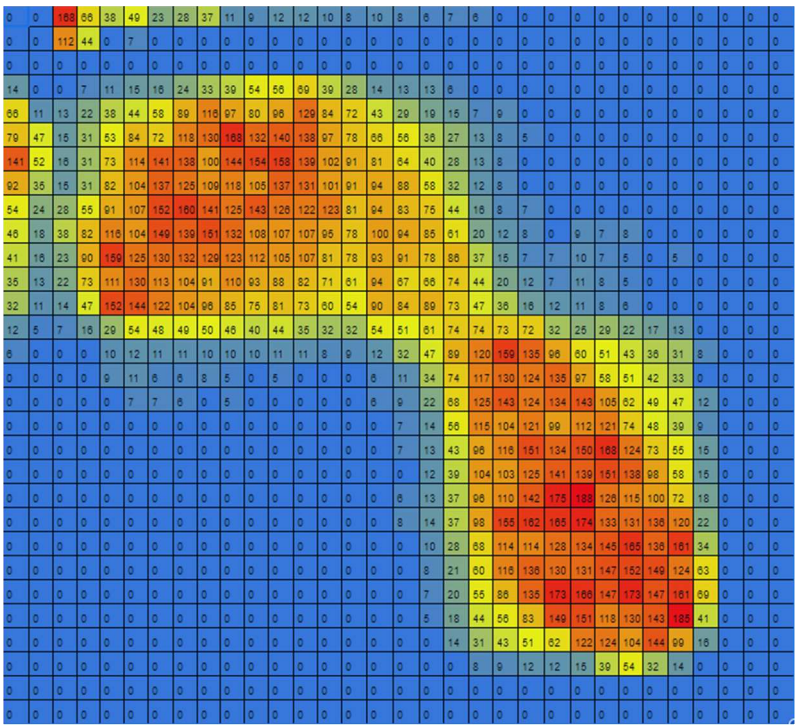


Figure 9. Coloring Data with Conditional Formatting

In Figure 9, all analog data read from the upper base is processed and colored. These plantar pressure values belong to a male individual who weighs 100kg, is 185cm tall, is 28 years old, and has a foot size of 43.

As a result of the study, plantar pressure measurement was achieved from 421 points using velostat nylon. When the measured values were examined, it was observed that the centers of the metatarsal and

tarsal regions on the sole of the foot were under high pressure. At the same time, these pressure values decrease with distance from the center.

In the literature review, plantar pressure measurement was achieved using two different methods: pressure platform and in-shoe systems [34]. Compared to studies in the literature, the results obtained in this study provide different advantages depending on the area of use.

In 2012, Razak et al. In the study conducted by A.Ş., the advantages and disadvantages of platform-based and in-shoe pressure measurement systems were compared. The study mentioned that platform-based devices are limited to the laboratory, and the resolution of intrafoot pressure meters is low due to the number of sensors [15].

In studies conducted on the in-shoe plantar pressure system, pressure points were generally kept low due to lack of space. For this reason, the resolution of the post-measurement values is quite low. These measurements are compared in Table 2 in terms of measurement resolution, measurement speed, and price parameters. The resolution of this study is lower than that of the platform-based pressure measurement studies in the literature. However, if we compare the area covered by the device, we will see that the prototype made in this study is 44 feet in size and thin in structure. Therefore, it can be used to measure in-shoe pressure.

Table 2. Comparison of Studies in the Literature

Authors	Measurement Resolution	Measurement Speed (ms-Hz)	Approximate Cost ($)
This Study	421 Point	480-2	25
Shu et al. [32]	6 Point	10-100	15
Saito et al. [35]	7 Point	1100-1	45
Praet and Louwerens[36]	9 Point	2-500	-
Chen et al.[37]	8 Point	20-50	37
Bamberg et al.[31]	5 Point	15-75	30
Pappas et al.[38]	3 Point	10-100	90
Healy et al.[30]	8 Point	10-100	40

When compared to studies in the literature, it has been observed that this study has a high resolution among in-shoe pressure measurement systems. Based on the measurement speed, it has a slower processing speed than many studies in the literature. The reason for this is the individual reading time of each sensor. When a cost-based comparison is made, a more cost-effective prototype has been developed compared to the majority of studies in the literature. When all variables are considered, it has been observed that the performance of the system implemented in this study is higher. No study on higher sensitivity in-shoe plantar pressure measurement was found in the reviewed literature. For this reason, the study can be recommended for biomedical studies, considering its high sensitivity and compact structure regarding in-shoe plantar pressure measurement.

REFERENCES

[1] D. Karaman, K. Dilek, and N. Y. Atar, "Evde sağlık hizmeti verilen bireylerin hastalık durumlarının ve bakım ihtiyaçlarının değerlendirilmesi: Zonguldak örneği", *Gümüşhane University Journal of Health Sciences*, vol. 4, issue 3, p. 347-359, 2015.

[2] B. Anafaroğlu, "Halluks valgus deformitesinin yaşam kalitesi üzerine etkisi", *Ankara Health Services Journal,* vol. 11, issue 1, p. 9-15, 2012.

[3] T. Karataş, E. Yılmaz, and Ü. Polat, "Osteoartrit Yönetimi, Yaşam Kalitesi ve Hemşirenin Destekleyici Rolü", *SDU Faculty of Medicine Journal*, vol. 29, issue 2, p. 265-271, 2022.

[4] T. Çankaya, "İlköğretim çağındaki çocuklarda ayak, ayak bileği deformitelerinin podoskop ile değerlendirilmesi", master's thesis, Bolu Abant İzzet Baysal University, Institute of Health Sciences, Bolu, Türkiye, 2004.

[5] Y. F. Shih, C. Y. Chen, W. Y. Chen, and H. C. Lin, "Lower extremity kinematics in children with and without flexible flatfoot: a comparative study", *BMC musculoskeletal disorders*, vol. 13, issue, p. 1-9, 2012.

[6] H. K. Sürmen, M. C. Fetvacı, I. Danışman, and Y. Z. Arslan, "Spina Bifida Hastalığı Olan Çocuklar İçin Ayak-Ayak Bileği Ortezi Tasarımı", doctoral thesis, Istanbul University Institute of Science and Technology, İstanbul, Türkiye, July 2016.

[7] Y. Güzel, "Diz Ağrılı Hastaya Yaklaşım", *Clinical Medicine Family Medicine*, vol. 9, issue 1, p. 27-32, 2017.

[8] H. Kaya, "Diz osteoartrit tanılı bireylerde denge ve plantar basıncın değerlendirilmesi", master's thesis, Istanbul Medipol University Institute of Health Sciences, İstanbul, Türkiye, 2020.

[9] C. Turan, "Karbon tabanlık kullanımının farklı ayak deformitelerindeki ayak plantar basınç dağılımına etkisi", master's thesis, Istanbul Medipol University Institute of Health Sciences, İstanbul, Türkiye, 2021.

[10] A. Selin and S. Çolak, "Üniversite öğrencilerinde ayak medial longitudinal ark durumunun denge ve esneklikle ilişkisi", *Acıbadem University Journal of Health Sciences*, vol. 11, issue 4, p. 625-630, 2020.
[11] B. Nemeth, "The diagnosis and management of common childhood orthopedic disorders", *Current problems in pediatric and adolescent health care*, vol. 41, issue 1, p. 2-28, 2011.
[12] E. J. Strandberg, T. Mozaffar and R. Gupta, "The role of neurodiagnostic studies in nerve injuries and other orthopedic disorders", *The Journal of hand surgery*, vol. 32, issue 8, p. 1280-1290, 2007.
[13] J. Hickman and C. Peters, "Hip pain in the young adult: diagnosis and treatment of disorders of the acetabular labrum and acetabular dysplasia", *American Journal of Orthopedics (Belle Mead, NJ)*, vol. 30, issue 6, p. 459-467, 2001.
[14] M. Morgenstern, R. Kühl, H. Eckardt, Y. Acklin, B. Stanic, M. Garcia, D. Baumhoer and W.J. Metsemakers, "Diagnostic challenges and future perspectives in fracture-related infection", *Injury*, vol. 49, issue, p. S83-S90, 2018.
[15] A. H. A. Razak, A. Zayegh, R.K. Begg, and Y. Wahab, "Foot plantar pressure measurement system: A review", *Sensors*, vol. 12, issue 7, p. 9884-9912, 2012.
[16] R. Periyasamy and S. Anand, "The effect of foot arch on plantar pressure distribution during standing", *Journal of medical engineering & technology*, vol. 37, issue 5, p. 342-347, 2013.
[17] S. Özyürek, İ. Demirbüken, Ö. Ç. Tosun, R. E. Okyay and S. Angın, "Gebelik sürecinde zaman mesafe parametreleri ve plantar basınç dağılımı", *Fizyoterapi Rehabilitasyon*, vol. 24, issue 1, p. 71-79, 2013.
[18] M.Lord, "Foot pressure measurement: a review of methodology", *Journal of biomedical engineering*, vol. 3, issue 2, p. 91-99, 1981.
[19] A. K. Buldt, S. Forghany, K. B. Landorf, P. Levinger, G. S. Murley and H. B. Menz, "Foot posture is associated with plantar pressure during gait: A comparison of normal, planus and cavus feet", *Gait & posture*, c. 62, sayı, ss. 235-240, 2018.
[20] C. Sungur, "Tıbbi Görüntüleme Hizmetlerinin Gereksiz Kullanımı ve Buna Karşı Çözüm Önerileri", *Kahramanmaraş Sütçü İmam University Faculty of Economics and Administrative Sciences Journal*, vol. 8, issue 1, p. 67-86, 2018.
[21] F. Duygulu, S. Mıstık, H. Şahan and A. Öztürk, "Aile Hekimliği Uzmanlık Eğitiminde Ortopedi ve Travmatoloji: Teşhis ve Tedavide Bilinmesi ve Uygulanması Gerekenler", *Tıp Eğitimi Dünyası*, vol. 18, issue 18, p. 27-31, 2005.
[22] R. Ferber, T. Webber, B. Everett and M. Groenland, "Validation of plantar pressure measurements for a novel in-shoe plantar sensory replacement unit", *Journal of diabetes science and technology*, vol. 7, issue 5, p. 1167-1175, 2013.
[23] A. Gefen, "Pressure-sensing devices for assessment of soft tissue loading under bony prominences: technological concepts and clinical utilization", *Wounds: a compendium of clinical research and practice*, vol. 19, issue 12, p. 350-362, 2007.
[24] B. MacWilliams and P. Armstrong, "Clinical applications of plantar pressure measurement in pediatric orthopedics", *Pediatric gait: a new millennium in clinical care and motion analysis technology*, p. 143-150, 2000.
[25] Y. Cong and M. Zhang. "Measurement of in-shoe plantar triaxial stresses in high-heeled shoes", *2010 3rd International Conference on Biomedical Engineering and Informatics*, p. 1760-1763, 2010.
[26] S. Urry, "Plantar pressure-measurement sensors", *Measurement science and technology*, vol. 10, issue 1, p. R16, 1999.
[27] W. Putnam and R. B. Knapp, "Input/data acquisition system design for human computer interfacing", *Unpublished Lecture Notes*, October, vol. 17, sayı, 1996.
[28] X. Li, K. Wang, Y.L. Wang and K. C. Wang, "Plantar pressure measurement system based on piezoelectric sensor: a review", *Sensor Review*, vol. 42, issue 2, p. 241-249, 2022.
[29] Y. Feng, Y. Ge and Q. Song. "A human identification method based on dynamic plantar pressure distribution", *2011 IEEE International Conference on Information and Automation*, p. 329-332, 2011.
[30] A. Healy, P. Burgess-Walker, R. Naemi and N. Chockalingam, "Repeatability of WalkinSense® in shoe pressure measurement system: A preliminary study", *The Foot*, vol. 22, issue 1, p. 35-39, 2012.
[31] S. J. M. Bamberg, A. Y. Benbasat, D. M. Scarborough, D. E. Krebs and J. A. Paradiso, "Gait analysis using a shoe-integrated wireless sensor system", *IEEE transactions on information technology in biomedicine*, vol. 12, issue 4, p. 413-423, 2008.
[32] L. Shu, T. Hua, Y. Wang, Q. Li, D. D. Feng and X. Tao, "In-shoe plantar pressure measurement and analysis system based on fabric pressure sensing array", *IEEE Transactions on information technology in biomedicine*, vol. 14, issue 3, p. 767-775, 2010.
[33] W. Liu, M. Zhang and X. Zhou, "The implement of multichannel and adjustable gain A/D sampling system", *2011 International Conference on Consumer Electronics, Communications and Networks (CECNet)*, p. 1819-1822, 2011.
[34] D. Rosenbaum and H. P. Becker, "Plantar pressure distribution measurements. Technical background and clinical applications", *Foot and ankle surgery*, vol. 3, issue 1, p. 1-14, 1997.
[35] W. Liu, M. Zhang and X. Zhou, "The implement of multichannel and adjustable gain A/D sampling system daily human activity", *Medical engineering & physics*, vol. 33, issue 5, p. 638-645, 2011.
[36] S. F. Praet and J. W. K. Louwerens, "The influence of shoe design on plantar pressures in neuropathic feet", *Diabetes care*, vol. 26, issue 2, p. 441-445, 2003.
[37] M. Chen, B. Huang, K. K. Lee and Y. Xu. "An intelligent shoe-integrated system for plantar pressure measurement", *2006 IEEE International Conference on Robotics and Biomimetics*, p. 416-421, 2006.
[38] I. P. Pappas, T. Keller, S. Mangold, M. R. Popovic, V. Dietz and M. Morari, "A reliable gyroscope-based gait-phase detection sensor embedded in a shoe insole", *IEEE sensors journal*, vol. 4, issue 2, p. 268-274, 2004.